

Therapeutic effect of a traditional Chinese medicine formulation on experimental choroidal neovascularization in mouse

Yu-Fei Zhang^{1,2}, Chuan Jiang^{1,3}, Xiao-Hong Zhou⁴, Dong-Yu Wei^{1,3}, Shao-Heng Li⁵, Pan Long⁶, Man-Hong Li⁷, Zuo-Ming Zhang^{1,3}, Tao Chen^{1,3}, Hong-Jun Du⁷

¹Center of Clinical Aerospace Medicine, Fourth Military Medical University, Xi'an 710032, Shaanxi Province, China

²The Air Force Hospital from Northern Theater PLA, Shenyang 110092, Liaoning Province, China

³Department of Aviation Medicine, Xijing Hospital, Fourth Military Medical University, Xi'an 710032, Shaanxi Province, China

⁴Ophthalmology, Children's Hospital of Fudan University, Shanghai 201102, China

⁵School of Basic Medicine, Fourth Military Medical University, Xi'an 710032, Shaanxi Province, China

⁶Department of Ophthalmology, General Hospital, Western Theater Command, Chengdu 610083, Sichuan Province, China

⁷Department of Ophthalmology, Xijing Hospital, Fourth Military Medical University, Xi'an 710032, Shaanxi Province, China

Co-first authors: Yu-Fei Zhang, Chuan Jiang, and Xiao-Hong Zhou
Correspondence to: Hong-Jun Du. No.127 Changlexi Road, Department of Ophthalmology, Xijing Hospital, Fourth Military Medical University, Xi'an 710032, Shaanxi Province, China. dhj2020@126.com; Tao Chen. No.169 Changlexi Road, Center of Clinical Aerospace Medicine, Fourth Military Medical University, Xi'an 710032, Shaanxi Province, China. ct1988@fmmu.edu.cn

Received: 2021-03-16 Accepted: 2021-06-11

Abstract

• **AIM:** To investigate therapeutic effects of traditional Chinese medicine formulations, Hexuemingmu (HXMM) on laser-induced choroidal neovascularization (CNV) and follow-up effect in mice.

• **METHODS:** C57BL/6 mice of 8-week-old were used and CNV was induced with 577 nm laser photocoagulation. Animals were randomly divided into groups and different doses of HXMM were administered daily. One, four, and eight weeks after the intervention, the electroretinogram (ERG), fundus fluorescence angiography, choroidal flat mount and immunofluorescence staining were performed to evaluate the function and CNV formation. The expression

levels of angiogenic proteins were determined by Western blotting and immunofluorescence staining. An analysis of variance and Kruskal-Wallis test were used to test the differences among the groups.

• **RESULTS:** The results showed that HXMM effectively increased amplitude of ERG of mice ($P < 0.05$), alleviated fundus CNV leakage ($P < 0.05$), and reduced the area of neovascularization and the expression of angiogenic proteins ($P < 0.05$) after laser-induced CNV.

• **CONCLUSION:** HXMM can protect the retinal function of mice after laser-induced CNV, and inhibit the CNV development.

• **KEYWORDS:** choroidal neovascularization; traditional Chinese medicine; mice

DOI: 10.18240/ijo.2021.10.04

Citation: Zhang YF, Jiang C, Zhou XH, Wei DY, Li SH, Long P, Li MH, Zhang ZM, Chen T, Du HJ. Therapeutic effect of a traditional Chinese medicine formulation on experimental choroidal neovascularization in mouse. *Int J Ophthalmol* 2021;14(10):1492-1500

INTRODUCTION

Choroidal neovascularization (CNV)-related diseases are major eye diseases that cause blindness, especially in many developed countries^[1-3]. They are characterized by pathological proliferative neovascularization and patients range from newborns to elder individuals, with a wide range of vulnerable populations. While the number of patients with of CNV-related diseases is increasing, there is currently no an ideal treatment. Symptomatic remission treatments such as anti-vascular endothelial growth factor (anti-VEGF) agents, laser photocoagulation, photodynamic therapy, and transpupillary thermotherapy are mainly used^[4-7].

CNV is the basic pathological change of many kinds of intraocular diseases and it often involves the macula and leads to serious damage of central vision^[8-9]. CNV comes from choroidal capillaries and invades retinal pigment epithelium (RPE) through Bruch's membrane. Due to the incomplete structure of CNV, the leakage fluid accumulates between RPE

Table 1 Ingredients of HXMM

Content ranking	Species names	Content ranking	Species names
1	Typhae Pollen	11	Prunellae Spica
2	Salviae Miltiorrhizae Radix et Rhizoma	12	Gentianae Radix et Rhizoma
3	Rehmanniae Radix	13	Curcumae Radix
4	Herba Ecliptae Eclipta prostrata L	14	Equisetum hyemale L.
5	Chrysanthemi Flos	15	Paeoniae Radix Rubra
6	Scutellariae Radix	16	Moutan Cortex
7	Cassiae Semen	17	Crataegi Fructus
8	Semen Plantaginis	18	Angelicae Sinensis Radix
9	Leonurus japonicus Houtt. Leonurus sibiricus L	19	Chuanxiong Rhizoma
10	Ligustri Lucidi Fructus		

layer and retina, which makes photoreceptor cells separate from RPE layer and eventually leads to blindness^[10]. Current studies show that the production of CNV is mainly related to VEGF, which can regulate vascular endothelial cells, promote angiogenesis and increase vascular permeability, therefore, VEGF and its receptor become the target molecules of CNV treatment^[11-12]. Study has shown that Hexuemingmu (HXMM) can regulate the level of VEGF in the eyes of rats with retinal central vein occlusion^[13]. With the development of traditional Chinese medicine (TCM) research, an increasing number of TCM formulations have been found to have good therapeutic effects on ophthalmic diseases that are difficult to treat conventionally^[13-14]. Therefore, as a traditional ophthalmic drug, can HXMM regulate VEGF to treat CNV? This study was to explore the potential therapeutic effects of HXMM on CNV-related diseases, with the aim of providing a novel therapeutic direction for these diseases.

MATERIALS AND METHODS

Ethical Approval All experiments were conducted in accordance with the Association for Research in Vision and Ophthalmology (ARVO) statement for the use of Animals in Ophthalmic and Vision Research. All procedures were carried in accordance with the Animal Research: Reporting *in vivo* Experiments (ARRIVE) guidelines.

Animals Ninety healthy adult male C57BL/6 mice (8-week-old) were obtained from the experimental animal center of the Fourth Military Medical University in Xi'an, Shaanxi Province, China (license No.SYXK 2017-0045). All animals were maintained under standard laboratory conditions, with food and water available *ad libitum*.

Choroidal Neovascularization Model The mice were anesthetized by intraperitoneal injection (IP) 1 mL/kg 1% sodium pentobarbital (Sigma-Aldrich, St Louis, MO, USA; P3761). After mydriasis with compound tropicamide eye drops (Santen Pharmaceutical Co., Ltd, Japan), six laser photocoagulation spots were made around the optic disc, with

1-2 disc diameters from it by using an image-guided laser system (577 nm) with specific parameters (power, 180 mW; duration, 100ms; spot size, 100 μ m)^[15]. Small bubbles accompanied by slight sound and no bleeding were regarded as the success of CNV inducing. The bilateral eyes of the mice were modeled using a laser.

Ingredients of Hexuemingmu The HXMM mainly includes the components in Table 1.

Grouping and Intervention After modeling, the mice were randomly divided into the following groups of 18 mice each control group, low-, moderate-, and high-dose (CG, LOW, MOD, and HIGH, respectively). In addition, a sham operation (Sham) group was set up. Except for laser modeling, other procedures on the Sham group were the same as those conducted on the CG. The CG and Sham groups were administered 10 mL/kg normal saline by gavage daily, whereas the LOW, MOD, and HIGH groups were administered intragastrically with HXMM (dissolved in 10 mL/kg normal saline) at doses of 0.34, 0.68, and 1.36 g/kg, respectively.

Electroretinography Electroretinography (ERG) was conducted 1, 4, and 8wk after drug administration. Six mice were randomly selected from each group at each time point and the ERG was performed in the right eyes of the experimental animals according to the standardized protocol of small animal ERG records established by ISCEV^[16]. Briefly, before the ERG, the mice were allowed to adapt to the dark overnight and then they were anesthetized by administering conventional IP injections of 3 mL/kg 1% pentobarbital sodium and 50 μ L 10% Lumianning II (Jilin Shengda Animal Pharmaceutical, Co., Ltd., Jilin Province, China).

Compound tropicamide eye drops were used to dilate the pupils and oxybuprocaine hydrochloride eye drops (Santen Pharmaceutical Co., Ltd., Japan) were used for corneal anesthesia. The electrodes were connected correctly and the action electrode was a silver-silver chloride (Ag-AgCl) corneal ring electrode. The reference and ground electrodes

were both stainless steel needle electrodes and were punctured under the cheek subcutaneous tissue and inserted into the tail subcutaneous tissue, respectively. The ERG was recorded under dim red light and at the end of the experiment, levofloxacin eye drops (Santen Pharmaceutical Co., Ltd., Japan) were administered for infection prevention.

Fluorescence Fundus Angiography Fluorescence fundus angiography (FFA) was performed 1, 4, and 8wk after drug administration. After the ERG, the animals were injected (IP) with 0.5 mL/kg 20% fluorescence solution (Baiyunshan Mingxing Corporation, Guangzhou, Guangdong Province, China) and FFA images were collected 1-2min later. The degree of fluorescence leakage was graded according to the method of Takehana *et al*^[17], and the classification criteria were as follows: no leakage, level 0; mild leakage, level 1; moderate leakage, level 2; and severe leakage level 3.

Choroidal Flat Mount After the completion of the *in vivo* experiment, the mice were anesthetized by IP injections with 6 mL/kg 1% pentobarbital, and dislocation of cervical vertebra was performed 5min later. The eyeballs of the mice were enucleated rapidly, immersed in 4% paraformaldehyde for 1h, and then the anterior segment and neuroretina were removed. After 4% paraformaldehyde fixation for 12h, four to six radial incisions were made on the choroidal complex. The rinse solution (0.2 mL Tween 20 and 0.5 g bovine serum albumin BSA dissolved in 100 mL phosphate-buffered saline, PBS, 0.1 mmol/L, pH 7.2) was used to rinse the choroidal complex 5 times for 5min.

Then, the choroidal complex was incubated with isolectin B4-fluorescein isothiocyanate (FITC) conjugate (Sigma-Aldrich, L2895, 10 µg/mL) at 4°C for 4h. The samples were sealed with glycerol and images of the choroidal flat mount were captured using a fluorescence microscope (BX53, Olympus, Japan).

Western Blot Analysis The choroidal tissues of the right eyeballs of the mice were separated and homogenized on ice in radioimmunoprecipitation assay (RIPA) buffer (Beyotime Institute of Biotechnology, Jiangsu, China), and proteinase/phosphatase inhibitors were added at a 1:100 ratio. Operation of electrophoresis was according to the protocol in our laboratory^[13].

The separated proteins were then transferred onto polyvinylidene fluoride (PVDF) membranes (Millipore, USA), which were incubated with 5% nonfat milk solution for 1h at 25°C, followed by incubation with the following antibodies: β-tubulin (1:1000, 2146s, Cell Signaling Technology), rabbit anti-hypoxia-inducible factor 1 (HIF-1) α antibody (1:250, bs-20399R; Bioss Biotechnology, Beijing, China), anti-VEGFA antibody (6 µg/mL; Ab1316, Abcam, Cambridge, MA, USA), and fibroblast growth factor (FGF)-2 antibody (1:500; sc-271847, Santa Cruz Biotechnology) overnight at 4°C.

After rinsing with PBS plus tween (PBST), the PVDF membranes were incubated with anti-rabbit immunoglobulin G (IgG), horseradish peroxidase (HRP)-linked (1:5000; 7074s; Cell Signaling Technology) and goat anti-mouse IgG(H+L) HRP (1:5000; 31430; Xianfeng Biotechnology Company, Shaanxi, China) antibodies at 25°C for 2h. After rinsing three times with PBST for 5min, an enhanced chemiluminescence solution (Millipore, USA) was used for protein visualization. The intensity of the immunoreactivity was quantified using densitometry using Quantity One software (Bio-Rad Laboratories, Inc., USA).

Histological Staining The left eyeballs of the mice were enucleated rapidly and immersed in a fixative solution (40% formaldehyde: distilled water: 95% ethanol: glacial acetic acid, 2:2:3:2) for 48h. The eyeballs were dehydrated, embedded in paraffin wax, and 4 µm thick sections were cut. The sections containing laser spots were chosen, stained with hematoxylin and eosin (H&E), and then observed under 400× magnification.

Immunofluorescence Staining The paraffin wax sections were dewaxed with xylene and hydrated using gradient ethanol. Sections were boiled with ethylenediaminetetraacetic acid (EDTA) antigen retrieval solution (Beyotime Institute of Biotechnology, Jiangsu, China) for 20min for antigen retrieval. The sections were washed with PBS after cooling to 25°C, blocked with 10% goat serum (Boster Biological Technology, Haimen, China) for 1h at 25°C, and then incubated with anti-VEGF antibody (1100; Ab1316, Abcam, Cambridge, MA, USA) overnight at 4°C.

After washing with PBST, sections were incubated with Alexa Fluor 594-conjugated goat anti-mouse IgG(H+L) (1:100; ZF-0512; ZSGB-BIO Biotechnology, Beijing, China) for 1h at 25°C. Antifade mounting medium with DAPI (Beyotime Institute of Biotechnology, Jiangsu, China) was used to seal the sections. Images of the sections were obtained using a laser scanning confocal microscope (Carl Zeiss AG, Germany).

Serum Biochemistry At 8wk after drug administration, blood samples were collected from the heart of each animal (before dislocation of cervical vertebra), centrifuged at 14 000 g for 20min at 4°C, and the supernatant was collected. The serum concentrations of aspartate transaminase (AST), alanine transaminase (ALT), uric acid (UA), blood urea nitrogen (BUN), and creatinine (CR) of the mice were detected using an automatic biochemical analyzer (Rayto Life Sciences Ltd., Shenzhen, China).

Statistical Analysis The IBM statistical package for the social science (SPSS) version 23.0 software (IBM, USA) was used for the statistical analysis. The normally distributed data were expressed as mean±standard error of the mean (SEM), whereas the abnormally distributed data were expressed as medians

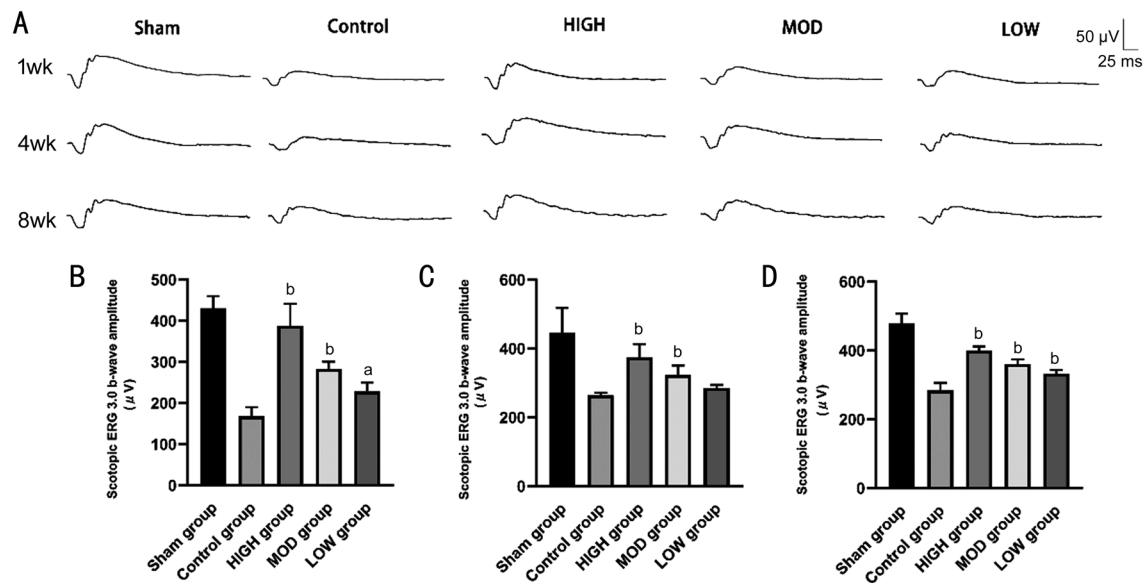


Figure 1 Hexuemingmu improved retinal function in mice with choroidal neovascularization A: Typical electroretinography (dark-adaptation response 3.0 b-wave) performance. Amplification of b-wave (dark-adaptation 3.0 response) after HXMM administration for 1 (B); 4 (C); and 8wk (D) in mice with CNV. Statistical significance was determined using one-way analysis of variance (ANOVA). Data are means±SEM. All analyses were performed in duplicate, $n=6$ mice per group. $^aP<0.05$ and $^bP<0.01$, intervention group vs control group.

Table 2 Grade of fundus fluorescence leakage in each group of experimental animals

Time of treatment	Groups	Level 3	Level 2	Level 1	Level 0	CNV leakage rate
1wk	CG	24	3	7	2	0.94
	LOW	16	10	6	4	0.88
	MOD	13	6	9	8	0.77
	HIGH ^b	8	10	11	7	0.80
4wk	CG	16	8	5	7	0.80
	LOW	16	8	9	3	0.91
	MOD	14	9	6	7	0.80
	HIGH	12	6	9	9	0.75
8wk	CG	21	8	4	3	0.91
	LOW	22	7	2	5	0.86
	MOD ^a	14	3	15	4	0.88
	HIGH ^b	7	12	12	5	0.86

Kruskal-Wallis test (H test) and Mann-Whitney U test; $n=36$; $^aP<0.05$ and $^bP<0.01$, intervention groups vs control group (CG).

and quartile [M (Q1, Q3)]. For normally distributed data, an analysis of variance (ANOVA), followed by Dunnett's post hoc analysis was performed to detect significant differences among the groups. For abnormally distributed data, the Kruskal-Wallis test (H test) and Mann-Whitney U test were performed to examine the significant differences among the groups. A $P\leq 0.05$ indicated statistical significance.

RESULTS

Effects of Hexuemingmu on Retinal Function of Choroidal Neovascularization Mice The objective examination of retinal function using ERG showed that compared with the Sham group, the retinal function of CNV mice in each experimental group was decreased. This finding was indicated by the decreased amplitude of scotopic 3.0 ERG response b-wave (Figure 1). Treatment with HXMM dose-dependently restored the amplitude of the scotopic 3.0 ERG response

b-wave in each treatment group, to a certain extent compared with that of the CG ($P<0.05$). Furthermore, 1wk after treatment, the difference between the treatment group and CG was the highest, and showed a stable time-dependent trend.

Reduction of Fundus Leakage by Hexuemingmu FFA was used to determine the effects of HXMM on leakage of the fundus. The FFA results showed that the CNV mice in the various groups exhibited different degrees of fluorescence leakage, and that of the HXMM-treated groups was significantly lighter than that of the CG was (Figure 2). The grading evaluation results of the analysis of fluorescence leakage intensity, showed that the CNV leakage rate and leakage intensity of the HIGH group was significantly lower than that of the CG after 1 and 8wk (Table 2, $P<0.05$), but not significantly at 4wk of treatment. In addition, the generation rate and leakage intensity of the MOD group was decreased

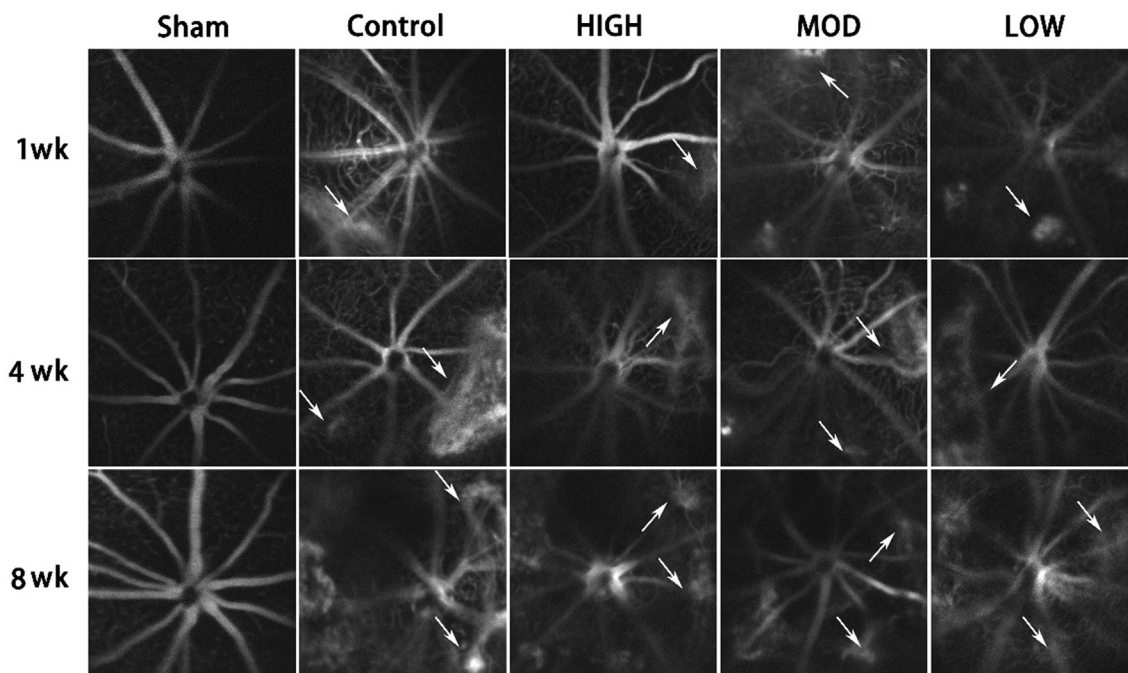


Figure 2 Typical fluorescence fundus angiography images of experimental animals White arrow: leakage point.

after 8wk of administration. However, the generation rate and leakage intensity of the CNV mice were not significantly changed by low-dose HXMM.

Effects of Hexuemingmu on Choroidal Neovascularization Leakage in Mice As shown in Figure 3, compared with the Sham group, CNV mice in each group showed different degrees of neovascularization around the laser spot (green light fluorescence). The area of neovascularization in the HXMM intervention groups was smaller than that in the CG, mainly at 1 and 8wk after administration.

Effects of Hexuemingmu on Pathological Changes in Choroidal Neovascularization Mice The Hematoxylin and eosin (H&E) staining (Figure 4) showed that after laser-induced CNV generation, the mouse retinas showed obvious damage, which manifested as a thinning or even disappearance of the outer nuclear layer, and the inner nuclear layer migrated to the injured area. The RPE and choroid were significantly thickened. The H&E staining also showed that the degree of choroidal thickening decreased with increasing doses of HXMM.

Effects of Hexuemingmu on Expression of Angiogenic Proteins in Choroidal Neovascularization Mice Detection of the expression of CNV-related proteins in the mouse choroid (Figure 5) showed high-dose HXMM continuously reduced the expression of VEGFA in the choroid ($P < 0.05$), whereas the effect of the moderate and small doses was only obvious at 1 and 4wk. In addition, the moderate- and high-dose HXMM continuously reduced the expression of FGF-2 protein in the choroid ($P < 0.05$), thereby alleviating the generation of CNV. However, the effect of HXMM on HIF-1 α expression was not obvious.

The distribution of VEGF expression in the eyeballs of mice was observed using immunofluorescence (Figure 6). The results demonstrated that the choroidal region of the normal mice showed low fluorescent staining. In contrast the laser-induced CNV mice showed strong fluorescence staining, and the stained region decreased with increasing HXMM dose.

Safety of Hexuemingmu The results of the serum biochemical tests (Figure 7) showed that 8wk administration of HXMM did not significantly affect the liver and kidney function of the mice, as indicated by the serum Cr, BUN, AST, ALT, and UA levels.

DISCUSSION

CNV is a type of abnormal vasculature originating from choroidal vessels, which is mainly caused by factors such as aging, trauma, inflammation, and tumors^[18-19]. The generation of CNV increases the permeability of the vascular. This process leads to increased susceptibility to bleeding, exudation, and scar formation and eventually leads to visual impairment and even blindness^[20]. The specific pathogenesis of CNV is unclear presently although numerous studies have shown that a variety of substances are closely related to its development. Among them, VEGF, FGF, epidermal growth factor (EGF), platelet-derived endothelial cell growth factor (PD-ECGF), and tumor necrosis factor (TNF) have been proved to play an important role in angiogenesis. VEGF is a soluble protein closely related to hypoxia that promotes vascular endothelial cell division, and has attracted much attention^[2,7]. It is a secreted polypeptide with specific mitotic effects on vascular endothelial cells and promote the proliferation and migration of endothelial cells. Therefore, VEGF plays a central role in

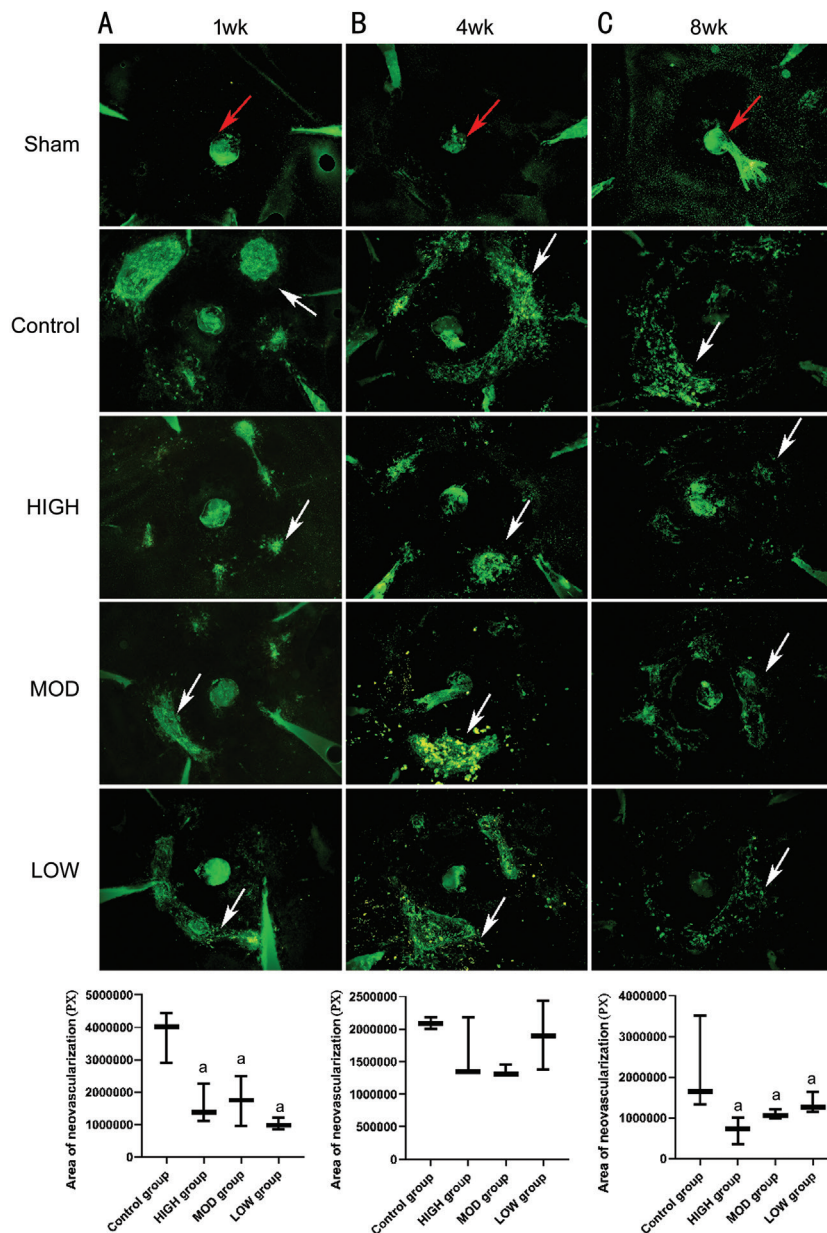


Figure 3 Typical choroidal stretched preparation images of mice White and red arrows indicate leakage point and optic disc, respectively. Area of choroidal neovascularization after Hexuemingmu administration for 1 (A); 4 (B); and 8wk (C) in mice with CNV. Statistical significance was determined using Kruskal-Wallis test (*H* test) and Mann-Whitney *U* test. Data are median and quartile range (M Q1, Q3); *n*=6 mice per group. ^a*P*<0.05, intervention groups vs control group.

CNV^[5-6]. FGF-2 is a multifunctional polypeptide that promotes angiogenesis, damage repair, and tissue regeneration^[21-23]. In retinal tissue, FGF-2 interacts with VEGF to play a role in promoting angiogenesis, and participates in the occurrence and development of retinal vascular diseases^[24].

The experimental CNV model is mainly established by the thermal, photochemical, and mechanical damage effects of a laser, which raises the local tissue temperature suddenly, causing protein denaturation, tissue damage, and cell necrosis^[1]. After RPE injury, local inflammatory reactions occur in the Bruch's membrane and choroid^[2]. In addition, a variety of growth factors and proteases secreted by the

inflammatory cells jointly promote the generation of CNV^[2]. We confirmed that treatment with HXMM effectively alleviated the various manifestations of laser-induced CNV generation in an established experimental CNV animal model. Our findings showed that treatment with HXMM effectively and in a dose-dependent manner, reduced the fluorescence leakage of the fundus, improved the electrophysiological function of retinal cells, and reduced the expression of related proteins to alleviate the manifestations of CNV. The generation of CNV is affected by many factors including VEGF, FGF, and HIF-1 α ^[25]. The results of our study showed that the expression of VEGF and FGF-2 in the choroid tissue was reduced by

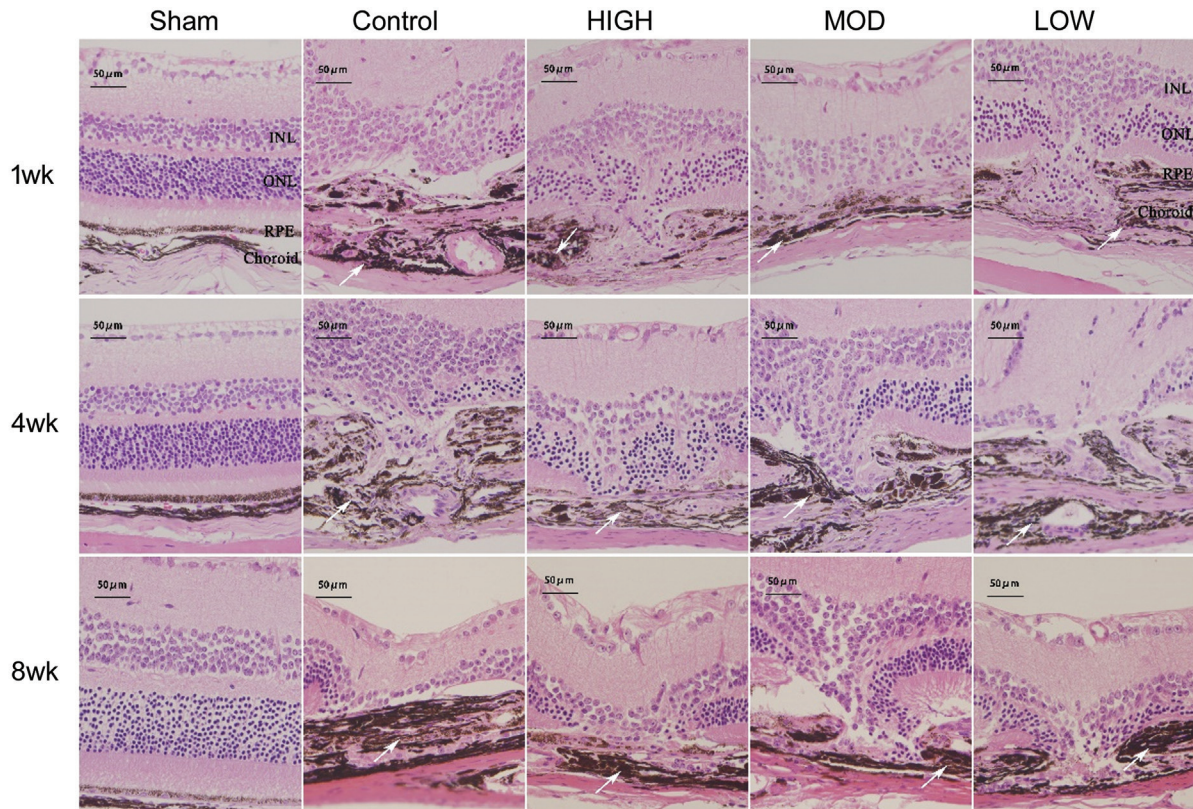


Figure 4 Hematoxylin and eosin images of mouse tissue samples White arrows: Thickened choroid. Outer nuclear layer thinned and the inner nuclear layer migrated to injured area. Pigment epithelium and choroid were significantly thickened and degree of choroidal thickening decreased in a Hexuemingmu (HXMM) dose-dependent manner.

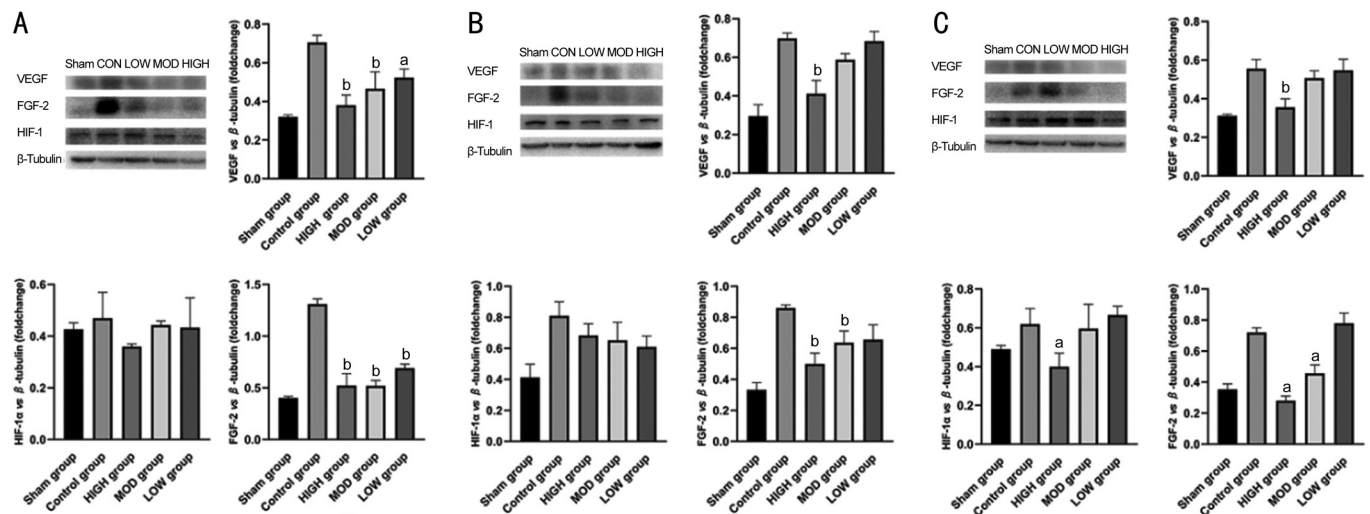


Figure 5 Hexuemingmu reduced expression of choroidal neovascularization (CNV)-related proteins Expression of CNV-related proteins after HXMM administration for 1 (A), 4 (B), and 8wk (C) in mice with CNV. Statistical significance determined using one-way analysis of variance. Data are means±SEM. All analyses were performed in duplicate, $n=6$ mice per group. ^a $P<0.05$ and ^b $P<0.01$, intervention groups vs control group.

treatment with HXMM in the early stage of CNV, which showed a more significant effect at a higher dose. However, in the late stage of CNV, HXMM protected visual function from CNV by inhibiting expression of FGF-2. Furthermore, a longer duration of treatment was used to ensure the safety. In addition, tanshinol and baicalin, the active components of HXMM,

have been shown to maintain the retinal microenvironment and improve retinal microcirculation^[26-27]. Studies have shown that baicalin improved vascular endothelial function and ameliorated vascular inflammation and oxidative stress^[28-30]. Moreover, HXMM protected the retina and promoted the absorption of retinal edema. Therefore, it restored the

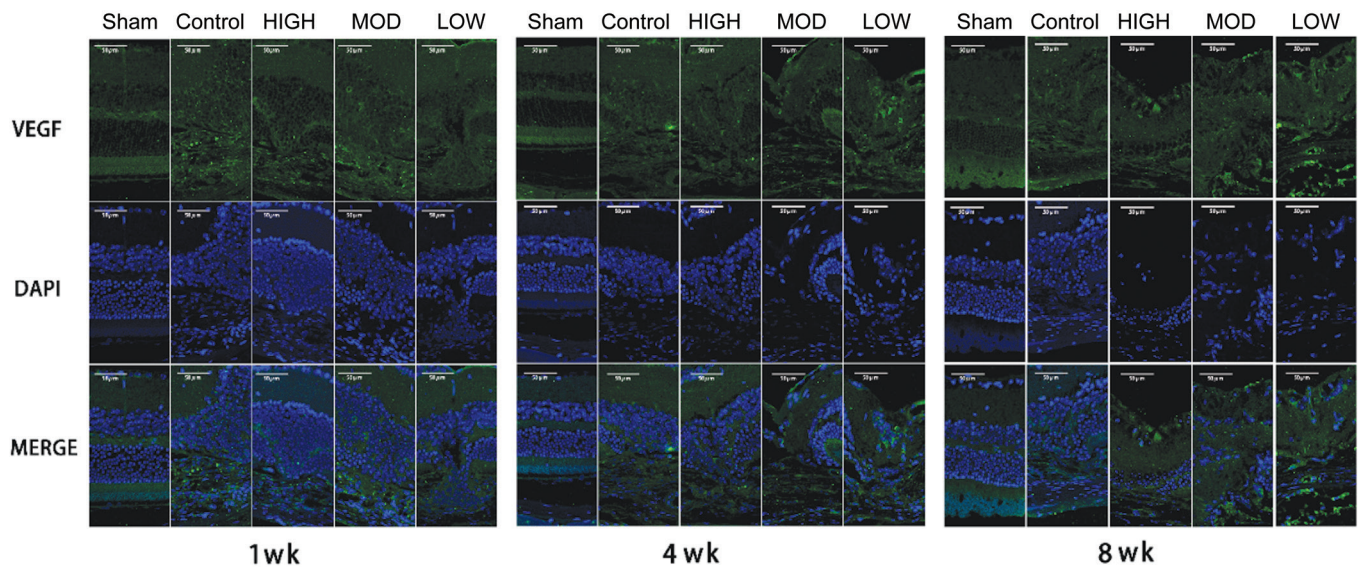


Figure 6 Vascular epidermal growth factor fluorescence staining images of mouse tissue samples Strong fluorescence signal of VEGF in injured area. Range of fluorescence staining region decreased with increasing Hexuemingmu dose.

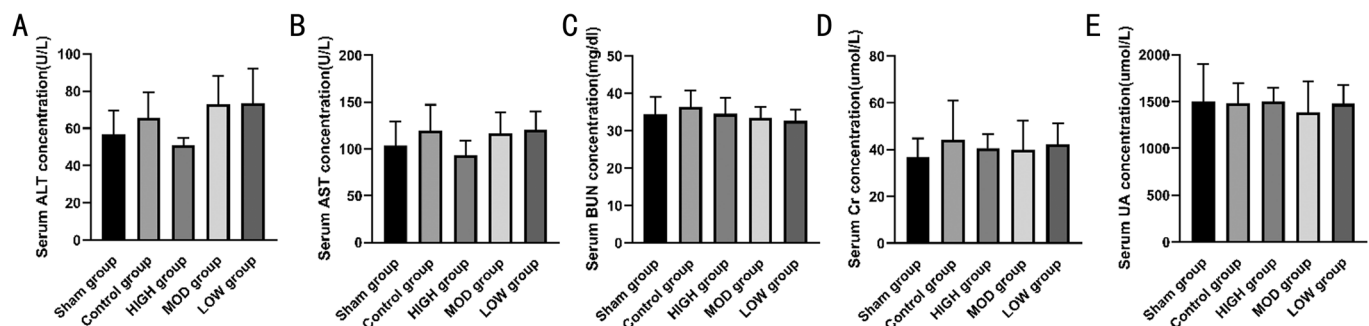


Figure 7 Hexuemingmu did not significantly affect liver and kidney function of mice Serum alanine transaminase (ALT; A); aspartate transaminase (AST; B); blood urea nitrogen (BUN; C); creatinine (Cr; D) and uric acid (UA; E) concentrations of mice with CNV. Statistical significance was determined using one-way analysis of variance. Data are means±SEM. All analyses were performed in duplicate, $n=5$ mice per group.

electrophysiological function of the retina and reduced the degree of fundal fluorescence leakage^[13].

In conclusion, this study confirmed that HXMM has a specific therapeutic effect on CNV in animal experiments. Its effect was mainly mediated by protecting the function of retinal cells, promoting the absorption of inflammatory exudation, and reducing the expression of related proteins. Our results provide a new reference for the treatment of CNV-related diseases.

ACKNOWLEDGEMENTS

The authors thank all those who have contributed to this study.

Foundation: Supported by the Army Laboratory Animal Foundation of China (No.SYDW2016-011).

Conflicts of Interest: Zhang YF, None; Jiang C, None; Zhou XH, None; Wei DY, None; Li SH, None; Long P, None; Li MH, None; Zhang ZM, None; Chen T, None; Du HJ, None.

REFERENCES

1 Chen YQ, Hahn P, Sloan FA. Changes in visual function in the elderly population in the United States: 1995-2010. *Ophthalmic Epidemiol* 2016;23(3):137-144.

2 Chan NS, Teo K, Cheung CM. Epidemiology and diagnosis of myopic choroidal neovascularization in Asia. *Eye Contact Lens* 2016;42(1): 48-55.

3 Sapielha P, Joyal JS, Rivera JC, Kermorvant-Duchemin E, Sennlaub F, Hardy P, Lachapelle P, Chemtob S. Retinopathy of prematurity: understanding ischemic retinal vasculopathies at an extreme of life. *J Clin Invest* 2010;120(9):3022-3032.

4 Kang EC, Seo JG, Kim BR, Koh HJ. Clinical outcomes of intravitreal bevacizumab versus photodynamic therapy with or without bevacizumab for myopic choroidal neovascularization: a 7-year follow-up study. *Retina* 2017;37(9):1775-1783.

5 Yan M, Huang Z, Lian HY, Song YP, Chen X. Conbercept for treatment of choroidal neovascularization secondary to pathologic myopia. *Acta Ophthalmol* 2019;97(5): e813-e814.

6 van Dijk EHC, van Rijssen TJ, Subhi Y, Boon CJF. Photodynamic therapy for chorioretinal diseases: a practical approach. *Ophthalmol Ther* 2020;9(2):329-342.

7 Rinaldi M, Semeraro F, Chiosi F, Russo A, Romano MR, Savastano MC, dell'Omo R, Costagliola C. Reduced-fluence verteporfin photodynamic

- therapy plus ranibizumab for choroidal neovascularization in pathologic myopia. *Graefes Arch Clin Exp Ophthalmol* 2017;255(3):529-539.
- 8 Feng LL, Ju MH, Lee KYV, MacKey A, Evangelista M, Iwata D, Adamson P, Lashkari K, Foxton R, Shima D, Ng YS. A proinflammatory function of toll-like receptor 2 in the retinal pigment epithelium as a novel target for reducing choroidal neovascularization in age-related macular degeneration. *Am J Pathol* 2017;187(10):2208-2221.
- 9 Zhao M, Xie WK, Tsai SH, Hein TW, Rocke BA, Kuo L, Rosa RH Jr. Intravitreal stanniocalcin-1 enhances new blood vessel growth in a rat model of laser-induced choroidal neovascularization. *Invest Ophthalmol Vis Sci* 2018;59(2):1125-1133.
- 10 Coughlin B, Schnabolk G, Joseph K, Raikwar H, Kunchithapautham K, Johnson K, Moore K, Wang Y, Rohrer B. Connecting the innate and adaptive immune responses in mouse choroidal neovascularization via the anaphylatoxin C5a and $\gamma\delta$ T-cells. *Sci Rep* 2016;6:23794.
- 11 Oshima Y, Oshima S, Nambu H, Kachi S, Hackett SF, Melia M, Kaleko M, Connelly S, Esumi N, Zack DJ, Campochiaro PA. Increased expression of VEGF in retinal pigmented epithelial cells is not sufficient to cause choroidal neovascularization. *J Cell Physiol* 2004;201(3):393-400.
- 12 Nochioka K, Okuda H, Tatsumi K, Morita S, Ogata N, Wanaka A. Hedgehog signaling components are expressed in choroidal neovascularization in laser-induced retinal lesion. *Acta Histochem Cytochem* 2016;49(2):67-74.
- 13 Long P, Yan WM, Liu JW, Li MH, Chen T, Zhang ZM, An J. Therapeutic effect of traditional Chinese medicine on a rat model of branch retinal vein occlusion. *J Ophthalmol* 2019;2019:9521379.
- 14 Liu HJ, Li X, Zhang ZD, Zeng JP, Dai Y, Wang C, Xie Z, Cheng L, Cui LR. Efficacy and safety of Bujing Yishi tablet for glaucoma with controlled IOP: study protocol for a multi-centre randomized controlled trial. *Trials* 2020;21(1):423.
- 15 Du HJ, Sun XF, Guma M, Luo J, Ouyang H, Zhang XH, Zeng J, Quach J, Nguyen DH, Shaw PX, Karin M, Zhang K. JNK inhibition reduces apoptosis and neovascularization in a murine model of age-related macular degeneration. *Proc Natl Acad Sci U S A* 2013;110(6):2377-2382.
- 16 McCulloch DL, Marmor MF, Brigell MG, Hamilton R, Holder GE, Tzekov R, Bach M. Erratum to: ISCEV Standard for full-field clinical electroretinography (2015 update). *Doc Ophthalmol* 2015;131(1):81-83.
- 17 Takehana Y, Kurokawa T, Kitamura T, Tsukahara Y, Akahane S, Kitazawa M, Yoshimura N. Suppression of laser-induced choroidal neovascularization by oral tranilast in the rat. *Invest Ophthalmol Vis Sci* 1999;40(2):459-466.
- 18 Grossniklaus HE, Green WR. Choroidal neovascularization. *Am J Ophthalmol* 2004;137(3):496-503.
- 19 Grossniklaus HE, Green WR. Pathologic findings in pathologic myopia. *Retina* 1992;12(2):127-133.
- 20 Adatia FA, Luong M, Munro M, Tufail A. The other CNVM: a review of myopic choroidal neovascularization treatment in the age of anti-vascular endothelial growth factor agents. *Surv Ophthalmol* 2015;60(3):204-215.
- 21 Masaki K, Sakai M, Kuroki S, Jo JI, Hoshina K, Fujimori Y, Oka K, Amano T, Yamanaka T, Tachibana M, Tabata Y, Shiozawa T, Ishizuka O, Hochi S, Takashima S. FGF2 has distinct molecular functions from GDNF in the mouse germline niche. *Stem Cell Reports* 2018;10(6):1782-1792.
- 22 McKenzie J, Smith C, Karuppaiah K, Langberg J, Silva MJ, Ornitz DM. Osteocyte death and bone overgrowth in mice lacking fibroblast growth factor receptors 1 and 2 in mature osteoblasts and osteocytes. *J Bone Miner Res* 2019;34(9):1660-1675.
- 23 Renaud-Gabardos E, Tatin F, Hantelys F, Lebas B, Calise D, Kunduzova O, Masri B, Pujol F, Sicard P, Valet P, Roncalli J, Chaufour X, Garmy-Susini B, Parini A, Prats AC. Therapeutic benefit and gene network regulation by combined gene transfer of apelin, FGF2, and SERCA2a into ischemic heart. *Mol Ther* 2018;26(3):902-916.
- 24 Yang QH, Zhang Y, Jiang J, Wu MM, Han Q, Bo QY, Yu GW, Ru YS, Liu X, Huang M, Wang L, Zhang XM, Fang JM, Li XR. Protective effects of a novel drug RC28-E blocking both VEGF and FGF₂ on early diabetic rat retina. *Int J Ophthalmol* 2018;11(6):935-944.
- 25 Hachana S, Fontaine O, Sapiéha P, Lesk M, Couture R, Vaucher E. The effects of anti-VEGF and kinin B1 receptor blockade on retinal inflammation in laser-induced choroidal neovascularization. *Br J Pharmacol* 2020;177(9):1949-1966.
- 26 Peng QH, Yao XL, Zeng ZC, Su RB, Wei YP. Effects of Huoxue Tongmai Lishui method on fundus fluorescein angiography of non-ischemic retinal vein occlusion: a randomized controlled trial. *J Chin Integr Med* 2009;7(11):1035-1041.
- 27 Zhou D, Wei WB, Yang CX, Ding N, Liu Y, He ML, Hou ZJ, Zhou JQ. Treatment of retinal vein occlusion in rabbits with traditional Chinese medicine Fufang XueShuan Tong. *Chin Med J (Engl)* 2010;123(22):3293-3298.
- 28 Lee W, Ku SK, Bae JS. Anti-inflammatory effects of Baicalin, Baicalein, and Wogonin *in vitro* and *in vivo*. *Inflammation* 2015;38(1):110-125.
- 29 Sun SJ, Wu XP, Song HL, Li GQ. Baicalin ameliorates isoproterenol-induced acute myocardial infarction through iNOS, inflammation, oxidative stress and P38MAPK pathway in rat. *Int J Clin Exp Med* 2015;8(12):22063-22072.
- 30 Wei XL, Zhu XY, Hu N, Zhang XQ, Sun TJ, Xu JY, Bian XH. Baicalin attenuates angiotensin II-induced endothelial dysfunction. *Biochem Biophys Res Commun* 2015;465(1):101-107.